Computers and Concrete, Vol. 5, No. 3 (2008) 175-194
DOI: http://dx.doi.org/10.12989/cac.2008.5.3.175

Numerical modeling of heterogeneous material

W. Puatatsananon*

Department of Civil Engineering, Ubon Ratchathani University, Thailand

V. Saouma‡

Department of Civil Engineering, University of Colorado at Boulder, USA

V. Slowik‡†

Hochschule für Technik, Wirtschaft and Kultur Leipzig (FH), Germany
(Received Agust 7, 2007, Accepted April 22, 2008)

Abstract. Increasingly numerical (finite element) modeling of concrete hinges on our ability to develop a representative volume element with all its heterogeneity properly discretized. Yet, despite all the sophistication of the ensuing numerical models, the initial discretization has been for the most part simplistic. Whenever the heterogeneity of the concrete is to be accounted for, a mesh is often manually crafted through the arbitrary inclusion of the particles (aggregates and/or voids) in an *ad-hoc* manner. This paper develops a mathematical strategy to precisely address this limitation. Algorithms for the random generation and placement of elliptical (2D) or ellipsoid (3D) inclusions, with possibly radiating cracks, in a virtual concrete model are presented. Collision detection algorithms are extensively used.

Keywords: composites; mesoconcrete; concrete; representative equivalent volume.

1. Introduction

Concrete is a particularly complex and heterogeneous material which is still not fully understood. Laboratory tests which could elucidate some of its most intriguing behavior are not always easy to perform, and (as is often done in numerous scientific endeavors) we often replace physical tests with numerical simulation. Numerical models, accounting for the heterogeneity of the concrete, have been used to investigate its effective elastic, thermal, and transport characteristics.

Numerical (finite element) simulation of concrete must begin with a numerical model (i.e. finite element mesh) which is representative of its heterogeneity through a representative volume element (RVE). Ideally, a granulometric curve distribution, such as the one of Fuller and Thompson (1907) should be emulated. This is a particularly difficult task in which various levels of simplifications have been adopted.

The critical role played by the aggregates in triggering the formation of crack propagation, and

* Professor
‡ Professor, E-mail: victor.saouma@colorado.edu
‡† Professor

thus a nonlinear response of the RVE, was first highlighted by the experimental work of Hsu, *et al.* (1963) and Slate and Olsefski (1963). On the other hand, the earliest work in numerical concrete can be traced to the work of Roelfstra, *et al.* (1985) which has set the stage to numerous subsequent "meso-concrete" (termed coined for the first time) simulation. The problem of mesh generation for numerical concrete is a particularly challenging task, and in the earliest work those meshes were essentially hand-crafted, i.e., they were not the result of a rigorous methodology which seeks to randomly place a properly scaled set of aggregates. Indeed, one of the earliest mesh developed by Willam, *et al.* (1989) does appear againin more recent work by Carol and López (2001) and Willam, *et al.* (2005). Most recently, Leite, *et al.* (2007) presented a model for the simulation of fracture in cementitious material based on a mathematical modeling of the heterogeneity which bears great similarity to the model proposed in this paper (albeit described in much less details).

Currently, amongst the most advanced models for heterogeneous concrete are those of Roberts and Garboczi (2002) and Cusatis, *et al.* (2003). Alternatively, very few papers have addressed exclusively the simulation of aggregate distribution. Zheng, *et al.* (2003) developed such a 2D model for circular aggregates, albeit not in the context of a finite element simulation, but to replicate the Fuller distribution.

To generate representative volume elements (RVE) of heterogeneous materials, we need to simulate the placing of concrete. In this process, particles are to be randomly placed inside a cylinder at random orientations. Clearly, particles can not overlap, hence there is a need to implement a collision detection mechanism. Furthermore, the viscosity of the cement ensures that there is a minimum distance between aggregates.

To address the aforementioned issues, this paper will develop a numerical algorithm to generate a 2D (rectangular) or 3D (hexagonal or cylindrical) representative volume element (RVE)

2. Mathematical model of the heterogeneity

In a 2D model, voids and inclusions are assumed to be elliptical in shape with a parametric representation. For collision detection, and for inclusions without or with one or two radiating cracks, we introduce the concept of Transformed Particle (TP).

In 2D, the TP is defined as an ellipse which completely surrounds the inclusion and its eventual cracks. This ellipse will in turn be characterized by its center (x_c^T, y_c^T), the length of its semi-major axis (a^T), the length of its semi-minor axis (b^T), and the rotational angle with respect to the x axis (α^T).

The transformed shapes and the characteristics of each inclusion type are summarized in Fig. 1 and in table 1 which identifies the four possible configurations: ellipse, crack, ellipse with one or two radiating cracks.

In 3D case, we define the TP as the sphere completely surrounding the inclusion or crack with the eventual cracks. The shpere is then in turn characterized by its center and radius. The transformed shapes and the characteristics of each inclusion type are summarized in Fig. 1 and in Table 2.

Ellipse: The analytical equation of an ellipse centered at (x_c, y_c) which major axis is at an angle α with respect to the x axis, Fig. 2, is given by

$$\frac{(x')^2}{a^2} + \frac{(y')^2}{b^2} = 1 \tag{1}$$

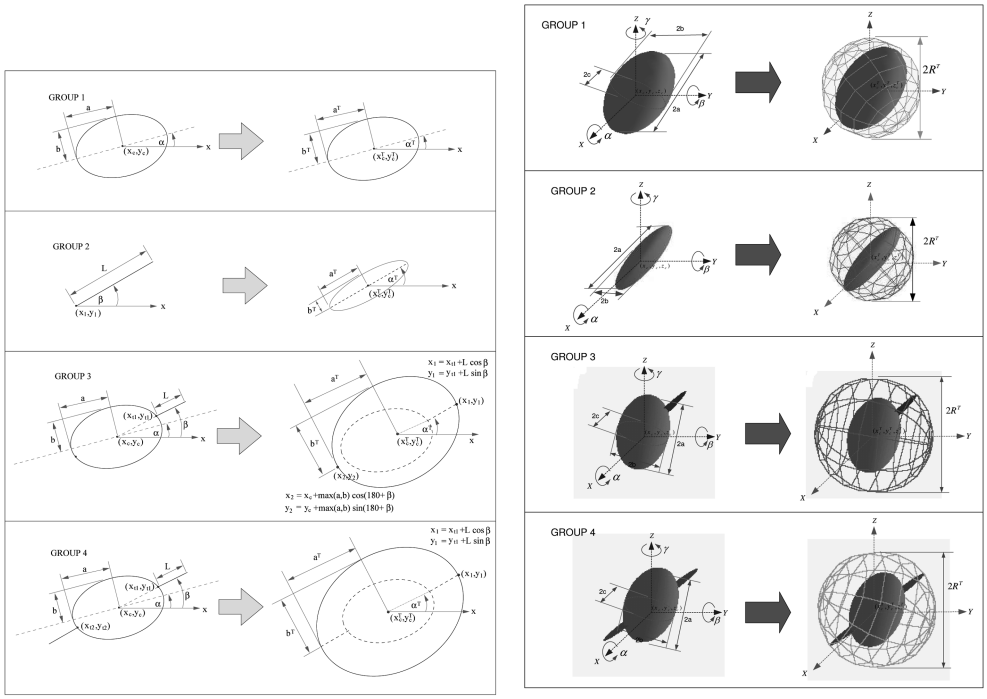

Fig. 1 2D and 3D particle transformation

Table 1 Parameters defining a TP in 2D

Type	x_c^T	y_c^T	a^T	b^T	α^T
1	x_c	y_c	a	b	α
2	$x_{t1}+\frac{L}{2}\cos\beta$	$y_{t1}+\frac{L}{2}\sin\beta$	$\frac{L}{2}$	user defines	β
3	$\frac{x_1+x_2}{2}$	$\frac{y_1+y_2}{2}$	$\frac{1}{2}\max(a,b)+\frac{1}{2}\sqrt{(x_1-x_c)^2+(y_1-y_c)^2}$	a	β
4	x_c	y_c	$\sqrt{(x_1-x_c)^2+(y_1-y_c)^2}$	max(a,b)	β

Table 2 Parameters defining a TP in 3D

Type	x_c^T	y_c^T	z_c^T	R^T
1	x_c	y_c	z_c	max (a, b, c)
2	x_c^{cr}	y_c^{cr}	z_c^{cr}	max (a^{cr}, b^{cr})
3	x_c	y_c	z_c	R^T
4	x_c	y_c	z_c	R^T

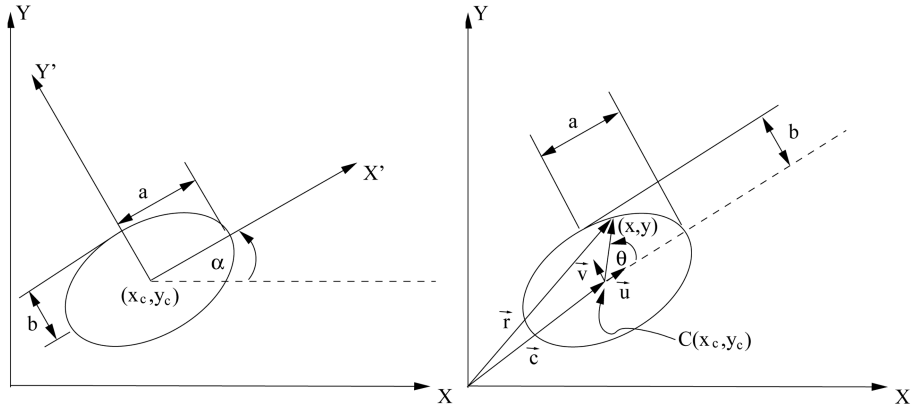

Fig. 2 General representation of an ellipse

where

$$\begin{Bmatrix} x' \\ y' \end{Bmatrix} = \begin{bmatrix} a_{11} & a_{12} \\ a_{21} & a_{22} \end{bmatrix} \begin{Bmatrix} x-x_c \\ y-y_c \end{Bmatrix} \tag{2}$$

where $a_{11} = \cos\alpha$, $\alpha_{12} = \sin\alpha$, $\alpha_{21} = -\sin\alpha$ and $\alpha_{22} = \cos\alpha$. Vectorially, the parametric equation of an ellipse is given by Fig. 2:

$$\vec{r} = \vec{c} + a\cos(\theta)\vec{u} + b\sin(\theta)\vec{v}, \quad \text{for } 0 \le \theta \le 2\pi \tag{3}$$

Ellipsoid: Similarly, the analytical equation of an ellipsoid centered at (x_c, y_c, z_c) with three rotational angles α, β and γ with respect to the x, y and z axes, respectively, Fig. 3 is given by:

$$\frac{(x')^2}{a^2} + \frac{(y')^2}{b^2} + \frac{(z')^2}{c^2} = 1 \tag{4}$$

where

$$\begin{Bmatrix} x' \\ y' \\ z' \end{Bmatrix} = \begin{bmatrix} a_{11} & a_{12} & a_{13} \\ a_{21} & a_{22} & a_{23} \\ a_{31} & a_{32} & a_{33} \end{bmatrix} \begin{Bmatrix} x-x_c \\ y-y_c \\ z-z_c \end{Bmatrix} \tag{5}$$

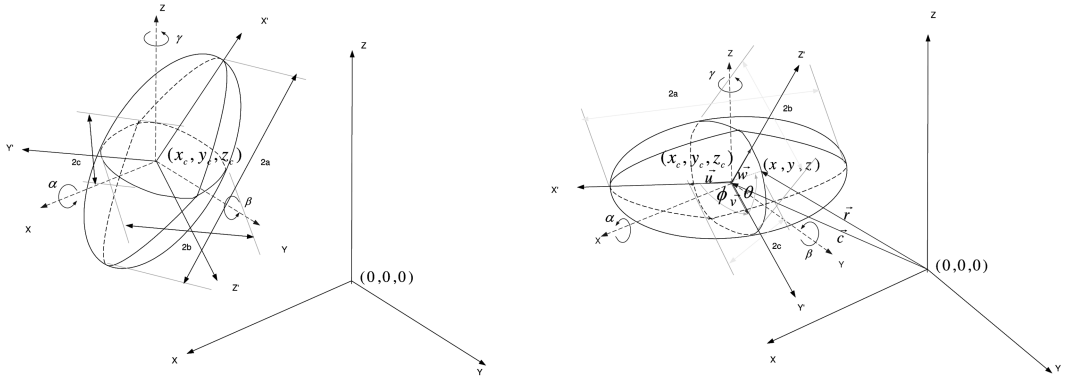

Fig. 3 General representation of ellipsoid

where

$$\begin{aligned}
a_{11} &= \cos\beta\cos\gamma \\
a_{12} &= -\cos\beta\sin\gamma \\
a_{13} &= \sin\beta \\
a_{21} &= \cos\alpha\sin\gamma + \sin\alpha\sin\beta\cos\gamma \\
a_{22} &= \cos\alpha\cos\gamma\sin - \sin\alpha\sin\gamma \\
a_{23} &= -\sin\alpha\cos\beta \\
a_{31} &= \sin\alpha\sin\gamma - \cos\alpha\sin\beta\cos\gamma \\
a_{32} &= \sin\alpha\cos\gamma + \cos\alpha\sin\beta\sin\gamma \\
a_{33} &= \cos\alpha\cos\beta
\end{aligned} \tag{6}$$

The corresponding parametric representation of the ellipsoid, Fig. 3, becomes

$$\begin{aligned}
\vec{r} &= \vec{c} + a\cos(\theta)\cos(\phi)\vec{u} + b\cos(\theta)\sin(\phi)\vec{v} \\
&+ c\sin(\theta)\vec{w} \quad \text{for} \quad -\frac{\pi}{2} \le \theta \le \frac{\pi}{2},\ -\frac{\pi}{2} \le \phi \le \frac{\pi}{2}
\end{aligned} \tag{7}$$

Sphere: The analytical equation of a sphere of radius r centered at the origin (0, 0, 0), is

$$x^2 + y^2 + z^2 = r^2 \tag{8}$$

In general, the sphere of radius r centered at (x_c, y_c, z_c) is represented by

$$(x - x_c)^2 + (y - y_c)^2 + (z - z_c)^2 = r^2 \tag{9}$$

3. Collision detection algorithms

Once the (randomly generated) location of each particle has been determined inside the RVE, we must ascertain that the transformed particle will not collide with either another one or a wall. If there is no collision, then we place the particle, otherwise the particle is shifted (as discussed below).

Hence, a collision detection algorithm must ensure that the distance between the transformed particle and another one (or a wall) is at least equal to the (user defined) minimum distance $D_{\min}$. To satisfy this physical requirement, the algorithm must determine if two entities (line or ellipse in 2D and plane or sphere in 3D) intersect, and the distance between them.

3.1. 2D formulation

3.1.1. Ellipse and line

Since the RVE is a rectangular entity, we must ascertain that there is no collision between a particle and the boundary (aggregate and cylinder).

Intersection: Given an ellipse characterized by the coordinates of its center (x_c, y_c), length of the semi-major axis = a, length of the semi-minor axis = b, and the orientation of its semi-major axis α with respect to the x axis and a vertical line defined by $x = x_1$ = constant, we first substitute $x = x_1$ into Eqs. (1), and (2) and simplify

$$Ay^2 + By + C=0 \tag{10}$$

where

$$A = \frac{a_{11}^2}{a^2} + \frac{a_{22}^2}{b^2}$$

$$B = \frac{2d_a a_{11}}{a^2} + \frac{2d_b a_{22}}{b^2} \tag{11}$$

$$C = \frac{a_a^2}{a^2} + \frac{d_b^2}{b^2} - 1$$

$$d_a = a_{11}x_1 - a_{11}x_c - a_{12}y_c$$

$$d_b = a_{21}x_1 - a_{21}x_c - a_{22}y_c$$

The y coordinates of the intersection points can be determined from Eq. (10)

$$y_{1/2} = \frac{-B \pm \sqrt{B^2 - 4AC}}{2A} \tag{12}$$

Hence, there will two intersection points if and only if

$$B^2 - 4AC \geq 0 \tag{13}$$

If $B^2 - 4AC = 0$, there will be only one intersection at $(x_1, -B/2A)$. The intersection between an ellipse and a horizontal line (y = constant) can be handled in a similar manner.

Distance: If there is no intersection between the ellipse and the line, we seek the distance between those two entities. For illustrative purposes, we restrict our self to the distance between an ellipse and a vertical line, Fig. 4.

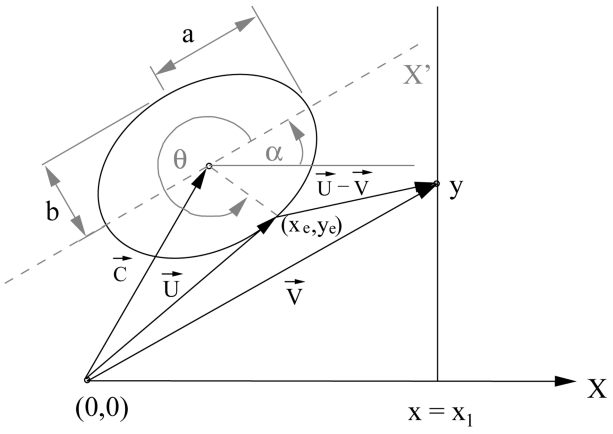

Fig. 4 Distance between an ellipse and a vertical line

We rewrite the parametric equation of the ellipse, Eq. (3), as

$$\vec{U} = \begin{Bmatrix} x_c \\ y_c \end{Bmatrix} + a \cos\theta \begin{Bmatrix} \cos\alpha \\ \sin\alpha \end{Bmatrix} + b \sin\theta \begin{Bmatrix} -\sin\alpha \\ \cos\alpha \end{Bmatrix} \tag{14}$$

while the one of the line is given by

$$\vec{V} = \begin{Bmatrix} x_1 \\ y \end{Bmatrix} \tag{15}$$

From Fig. 4, the distance between the ellipse and the line is given by

$$D = \left|\vec{V} - \vec{U}\right| \tag{16}$$

We define the function F as half of the squared distance D

$$F = \frac{1}{2}\left|\vec{V}(y) - \vec{U}(\theta)\right|^2 \tag{17}$$

Hence, the problem of determining the (minimum) distance between the ellipse and the line is recast as the determination of y and θ which minimize the function F in Eq. (17), or

$$\frac{\partial F}{\partial y} = (\vec{V} - \vec{U}) \cdot \frac{\partial \vec{V}}{\partial y} = 0$$

$$\frac{\partial F}{\partial \theta} = -(\vec{V} - \vec{U}) \cdot \frac{\partial \vec{U}}{\partial \theta} = 0 \tag{18}$$

We thus have a system of two (nonlinear) equations in terms of two unknowns (y and θ). The Newton-Raphson method, (Press, *et al.* 1988) is used to solve this nonlinear problem. Once we determine the two variables, then coordinate (x_e, y_e) of the point having the angle θ from the local X' axis on the ellipse can be determined and the actual distance d can be simply determined from $d = \sqrt{(x_e - x_1)^2 + (y_e - y)^2}$

3.1.2. Two ellipses

Intersection: Given two ellipses, E_1 and E_2 characterized by center point (x_{ci}, y_{ci}), the 2 semi axes (a_i, b_i) and the rotational angle α_i, (i=1, 2). We assume that a_2 is the longest of the semi-major axis, and hence ensure that E_2 can not lie entirely inside E_1. As will be shown later, we place the inclusions in ascending order (of size) inside the RVE.

To test for the intersection of two ellipses, we must determine if one of the ellipses is not fully contained by the other, or if the two ellipses intersect at two points.

• Ellipse Embedded into another:

We first check if E_1 is not fully inside E_2. We substitute Eq. (2) into Eq. (1), rearranging the equation we obtain

$$f = Ax^2 + By^2 + Cxy + Dx + Ey + F \tag{19}$$

where

$$A = \frac{c^2}{a_2^2} + \frac{s^2}{b_2^2}$$

$$B = \frac{s^2}{a_2^2} + \frac{c^2}{b_2^2}$$

$$C = \frac{2sc}{a_s^2} - \frac{2sc}{b_2^2}$$

$$D = -\frac{2x_{c2}c^2}{a_2^2} - \frac{2y_{c2}sc}{a_2^2} + \frac{2y_{c2}sc}{b_2^2} - \frac{2x_{c2}s^2}{b_2^2}$$

$$E = -\frac{2y_c c^2}{b_2^2} - \frac{2x_{c2}sc}{a_2^2} + \frac{2x_{c2}sc}{b_2^2} - \frac{2y_{c2}s^2}{a_2^2}$$

$$F = \frac{x_{c2}^2 c^2}{a_2^2} + \frac{y_{c2}^2 c^2}{b_2^2} + \frac{2x_{c2}sc}{b_2^2} - \frac{2y_{c2}s^2}{a_2^2} - \frac{2x_{c2}y_{c2}sc}{b_2^2} + \frac{x_{c2}^2 s^2}{b_2^2} + \frac{2x_{c2}y_{c2}sc}{a_2^2} - 1$$

$$c = \cos\alpha_2$$

$$s = \sin\alpha_2 \tag{20}$$

Then, to determine whether the center of E_1 is inside E_2, f in Eq. (19) is evaluated by substituting x, y with x_{c1}, y_{c1}. If f is less than or equal to zero, the center of E_1 is inside E_2, otherwise, it is outside.

• E_1 and E_2 are separated

If the center of an ellipse is not inside the other one, then to test for intersection we must first perform a so-called preparatory transformation process, Fig. 5:

1. Transform E_2 into a unit circle
2. Transform E_1 into the coordinate system of the transformed ellipse E_2 in step 1
3. Rotate the coordinate system of the transformed E_2 until the the axes of E_1 are parallel to the new coordinate axes.

Following the preparatory transformation process, we do have a new coordinate system in which E_2 is now a unit circle which has its center at the origin and E_1 remains an ellipse. Therefore, checking intersection of two ellipses is reduced to checking the intersection of the unit transformed circle E_2 and the transformed ellipse E_1 in the new coordinate system.

From Fig. 5, we assign $x_i y_i$ as the local coordinate systems for ellipse E_i. Therefore, the equation of the ellipse E_1 and E_2, in their respective local coordinate systems, is given by

$$\frac{x_1^2}{a_1^2} + \frac{y_1^2}{b_1^2} = 1 \tag{21}$$

$$\frac{x_2^2}{a_2^2} + \frac{y_2^2}{b_2^2} = 1 \tag{22}$$

Hence, the preparatory process proceeds as follows:

1. Transformation of E_2 into a unit circle: We first define the new coordinate system $x_2' - y_2'$,

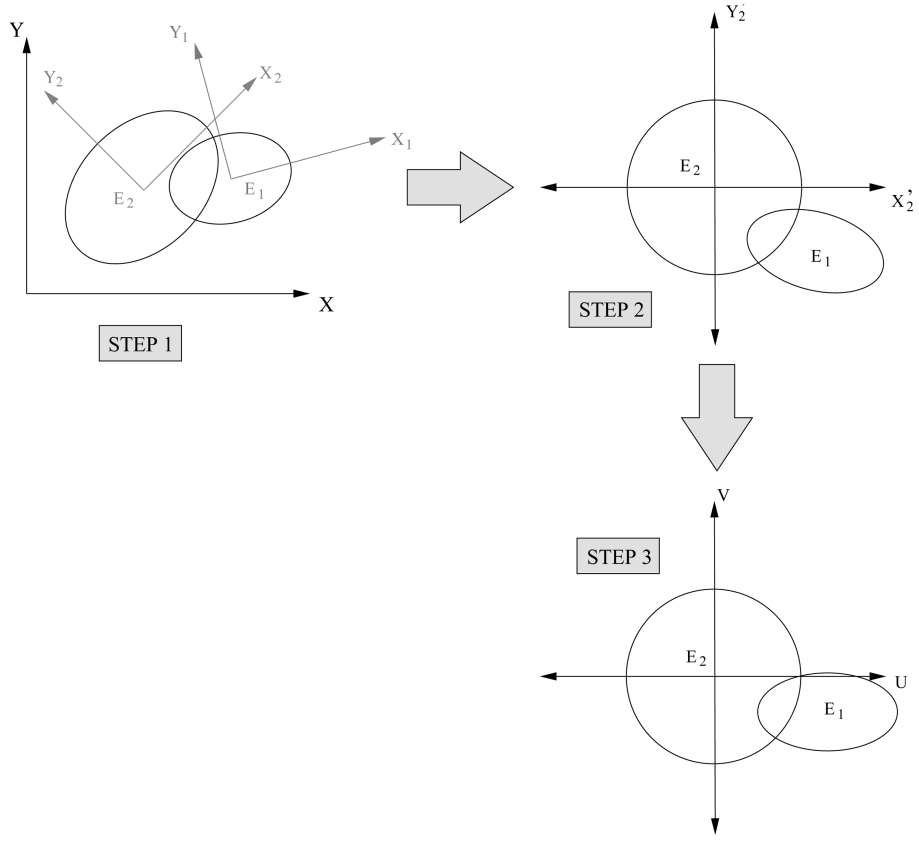

Fig. 5 Preparatory Transformation Process

related to the original one x_2y_2 through

$$x_2 = a_2x_2' \qquad y_2 = b_2y_2' \tag{23}$$

Then substituting x_2 and y_2 in Eq. (23) into Eq. (22), we obtain

$$(x_2')^2 + (y_2') = 1 \tag{24}$$

Eq. (22) of ellipse E_2 is now transformed into the one of a unit circle Eq. (24) in $x_2'-y_2'$ coordinate system, Fig. 5.

2. Transform E_1 into the coordinate system of the transformed ellipse E_2: Ellipse E_1 is now transformed into the coordinate system $x_2'-y_2'$ as follows

$$\begin{Bmatrix} x_1 \\ y_1 \end{Bmatrix} = \begin{bmatrix} c_1 & s_1 \\ -s_1 & c_1 \end{bmatrix} \left[\begin{bmatrix} c_2 & -s_2 \\ s_2 & c_2 \end{bmatrix} \begin{Bmatrix} a_2x_2' \\ b_2y_2' \end{Bmatrix} + \begin{Bmatrix} x_{c2}-x_{c1} \\ y_{c2}-y_{c1} \end{Bmatrix} \right] = \begin{Bmatrix} p_1x_2' + q_1y_2' + r_1 \\ p_2x_2' + q_2y_2' + r_2 \end{Bmatrix} \tag{25}$$

where

$$
\begin{aligned}
c_1 &= \cos\alpha_1 \\
s_1 &= \sin\alpha_1 \\
c_2 &= \cos\alpha_2 \\
s_2 &= \sin\alpha_2 \\
p_1 &= c_1\, c_2\, a_2 + s_1\, s_2\, a_2 \\
q_1 &= s_1\, c_2\, b_2 - c_1\, s_2\, b_2 \\
r_1 &= c_1\, x_{c_2} - c_1\, x_{c_1} + s_1\, y_{c_2}\, s_1\, y_{c_1} \\
p_2 &= c_1\, s_2\, a_2 - s_1\, c_2\, a_2 \\
q_2 &= s_1\, s_2\, b_2 + c_1\, c_2\, b_2 \\
r_2 &= -s_1\, x_{c_2} + s_1\, x_{c_1} + c_1\, y_{c_2} - c_1\, y_{c_2}
\end{aligned}
\tag{26}
$$

Then, substitute values of x_1 and y_1 in Eq. (25) into Eq. (21) and rearrange it. We will then obtain the equation of the transformed ellipse E_1 in the coordinate system $x_2'-y_2'$ asgiven by

$$A_{11}(x_2')^2 + A_{22}(y_2')^2 + 2A_{12}x_2'y_2' + B_1x_2' + B_2y_2' + C_1 = 0 \tag{27}$$

where

$$
\begin{aligned}
A_{11} &= \frac{p_1^2}{a_1^2} + \frac{p_2^2}{b_1^2} \\
A_{22} &= \frac{q_1^2}{a_1^2} + \frac{q_2^2}{b_1^2} \\
2A_{12} &= \frac{2p_1q_1}{a_1^2} + \frac{2p_2q_2}{b_1^2} \\
B_1 &= \frac{2p_1r_1}{a_1^2} + \frac{2p_2r_2}{b_1^2} \\
C_1 &= \frac{r_1^2}{a_1^2} + \frac{r_2^2}{b_1^2} - 1
\end{aligned}
\tag{28}
$$

3. Rotate the coordinate system: rotate the coordinate system $x_2'-y_2'$ until the coordinate axes becomes parallel to the ellipse E_1's axes. From Eq. (27) if $A_{12}\neq 0$, then the coordinate system $x_2'-y_2'$ can be rotated until the coordinate axes becomes parallel to the ellipse E_1's axes by determining the eigenvalues λ_1,λ_2 and corresponding normalized eigenvectors

$$e_1 = (e_{11}, e_{21}) \text{ and } e = (e_{12}, e_{22}) \text{ of } \begin{bmatrix} A_{11} & A_{12} \\ A_{12} & A_{22} \end{bmatrix}$$

and then defining the new coordinate system UV which is related to coordinate system $x_2'-y_2'$ through

$$\begin{Bmatrix} x_2' \\ y_2' \end{Bmatrix} = \begin{bmatrix} e_{11} & e_{12} \\ e_{21} & e_{22} \end{bmatrix} \begin{Bmatrix} u \\ v \end{Bmatrix} \tag{29}$$

Substituting x_2' and y_2' in Eq. (29) into Eq. (27), we obtain

$$\lambda_1 u^2 + \lambda_2 v^2 + \overline{B}_1 u + \overline{B}_2 v + C_1 = 0 \tag{30}$$

where

$$\begin{aligned} \overline{B}_1 &= B_1 e_{11} + B_2 e_{21} \\ \overline{B}_2 &= B_1 e_{12} + B_2 e_{22} \end{aligned} \tag{31}$$

Rearraging Eq. (30), we obtain

$$\lambda_1 \left(u + \frac{\overline{B}_1}{2\lambda_1} \right)^2 + \lambda_2 \left(v + \frac{\overline{B_2}}{2\lambda_2} \right)^2 - \overline{C} = 0 \tag{32}$$

where

$$\overline{C} = \frac{\overline{B}_1^2}{4\lambda_1^2} + \frac{\overline{B}_2^2}{4\lambda_2^2} - C_1 \tag{33}$$

or

$$\frac{\left(u + \frac{\overline{B}_1}{2\lambda_1} \right)^2}{\frac{\overline{C}}{\lambda_1}} + \frac{\left(v + \frac{\overline{B}_2}{2\lambda_2} \right)}{\frac{\overline{C}}{\lambda_2}} - 1 = 0 \tag{34}$$

Hence, the ellipse E_1 in the new coordinate UV has center coordinates

$$(u_c, v_c) = \left(-\frac{\overline{B}_1}{2\lambda_1}, -\frac{\overline{B}_2}{2\lambda_2} \right) \tag{35}$$

where one semi axis length is given by

$$\overline{a} = \sqrt{\frac{\overline{C}}{\lambda_1}} \tag{36}$$

along direction $\vec{e_1}$=(e_{11}, e_{21}) and the other axis length is given by

$$\overline{b} = \sqrt{\frac{\overline{C}}{\lambda_2}} \tag{37}$$

along direction $\vec{e_2}$=(e_{12}, e_{22})

Following this prepatory process, both ellipses are now in the new coordinate system shown in step 3 of Fig. 5.

Now, we can proceed to test the intersection of the 2 ellipses by checking the intersection of the transformed unit circle E_2 and the transformed ellipse E_1. The equation of the transformed unit circle E_2 is given by

$$u^2 + v^2 = 1 \tag{38}$$

We thus substitute $u = \sqrt{1 - v^2}$ from Eq. (38) into Eq. (34) and rearrange

$$P_1 v^2 + P_2 v + P_3 = P_4 \sqrt{1 - v^2} \tag{39}$$

where

$$\begin{aligned} P_1 &= \bar{a}^2 - \bar{b}^2 \\ P_2 &= -2\bar{a}^2 v_c \\ P_3 &= \bar{b}^2 - \bar{a}^2\bar{b}^2 + \bar{b}^2 u_c^2 + \bar{a}^2 v_c^2 \\ P_4 &= -2\bar{b}^2 u_c \end{aligned} \tag{40}$$

We now have a nonlinear equation in terms of v in Eq. (39) and it is again solved by the Newton-Raphson Method (Press, *et al*. 1988). If a solution does exist, the two ellipses intersect, otherwise, there is no intersection between the 2 ellipses.

Distance: Next we seek to determine the distance between the two ellipses E_1 and E_2 using a procedure similar to the one adopted to determine the shortest distance between an ellipse and a line.

With reference to Fig. 6 we begin with the parameteric representation of the two ellipses

$$\vec{U} = \begin{Bmatrix} x_{c1} \\ y_{c1} \end{Bmatrix} + a_1 \cos\theta_1 \begin{Bmatrix} \cos\alpha_1 \\ \sin\alpha_1 \end{Bmatrix} + b_1 \sin\theta_1 \begin{Bmatrix} -\sin\alpha_1 \\ \cos\alpha_1 \end{Bmatrix} \tag{41}$$

$$\vec{V} = \begin{Bmatrix} x_{c2} \\ y_{c2} \end{Bmatrix} + a_2 \cos\theta_2 \begin{Bmatrix} \cos\alpha_2 \\ \sin\alpha_2 \end{Bmatrix} + b_2 \sin\theta_2 \begin{Bmatrix} -\sin\alpha_2 \\ \cos\alpha_2 \end{Bmatrix} \tag{42}$$

The shortest distance between the 2 ellipses is thus given by

$$D = \left|\vec{V} - \vec{U}\right| \tag{43}$$

We again define a function F which is half of the squared distance D and is given by

$$F = \frac{1}{2}\left|\vec{V}(\theta_1) - \vec{U}(\theta_2)\right|^2 \tag{44}$$

To determine the distance between 2 ellipses, F must be minimized, and such a minimization exists if

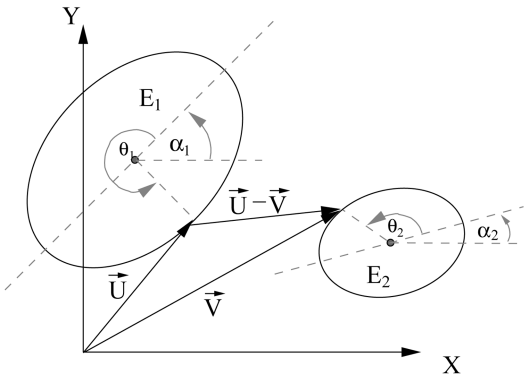

Fig. 6 Distance between 2 ellipses

$$\frac{\partial F}{\partial \theta_1} = (\vec{V}-\vec{U})\cdot\frac{\partial \vec{V}}{\partial \theta_1} = f_1(\theta_1, \theta_2) = f_1(c_1, s_1, c_2, s_2) = 0 \tag{45}$$

and

$$\frac{\partial F}{\partial \theta_2} = -(\vec{V}-\vec{U})\cdot\frac{\partial \vec{V}}{\partial \theta_2} = f_2(\theta_1, \theta_2) = f_2(c_1, s_1, c_2, s_2) = 0 \tag{46}$$

where c_1, s_1, c_2, and s_2 are equal to $\cos\theta_1$, $\sin\theta_1$, $\cos\theta_2$, and $\sin\theta_2$, respectively.

To solve for θ_1 and θ_2, we need two additional equations

$$f_3(c_1, s_1) = c_1^2 + s_1^2 = 0 \tag{47}$$

$$f_4(c_2, s_2) = c_2^2 + s_2^2 = 1 \tag{48}$$

Eqs. (45)-(48) constitute a set of nonlinear equations which will again be solved through the Newton-Raphson method, (Press, *et al.* 1988), to determine c_1, s_1, c_2, and s_2. Once those are obtained, we can easily determine θ_1 and θ_2, the coordinates of the points on both ellipses which have the shortest distance between them, and the actual distance between the 2 ellipses.

3.2. 3D Formulation

3.2.1. Sphereand REV surface

The sphere (bounded particle) shouldn't intersect with surface of the REV and at least should have the minimum distance $D_{\min}$ from the surface. Consider the sphere represented by its center (x_c, y_c, z_c) and its radius (r). Checking for the intersection and the minimum distance between the sphere and both types of REV surface, box and cylinder, are considered in this section.

Box surface: The intersection of the sphere and a plane parallel to *yz* plane is first considered. The plane is defined by $x-x_1=0$. Hence, intersection occurs if $x_c + r + D_{\min} \geq x_1$ The equations for checking the intersection of the sphere and the other box surface and their minimum distance are summarized in Table 3.

From Fig. 7(a), the intersection of the given sphere with the surface can be checked by considering the intersection of the sphere and the surface in the plane of $z = z_c$ as shown in Fig. 7(b). The equation of the intersection is given by

$$d + r \geq R \tag{49}$$

where d is a distance from the origin to the center of the sphere. The sphere should have at least

Table 3 Equations for checking the intersection of the sphere and the box surface and their minimum distance

Plane	Intersection Equation	Minimum Distance Equation
x=0	$x_c - r \leq 0$	$x_c - r - D_{\min} \leq 0$
x=W	$x_c + r \geq W$	$x_c + r + D_{\min} \geq W$
y=0	$y_c - r \leq 0$	$x_c - r - D_{\min} \leq 0$
z=0	$z_c - r \leq L$	$x_c - r - D_{\min} \leq 0$
z=H	$z_c + r \geq H$	$x_c + r + D_{\min} \geq H$

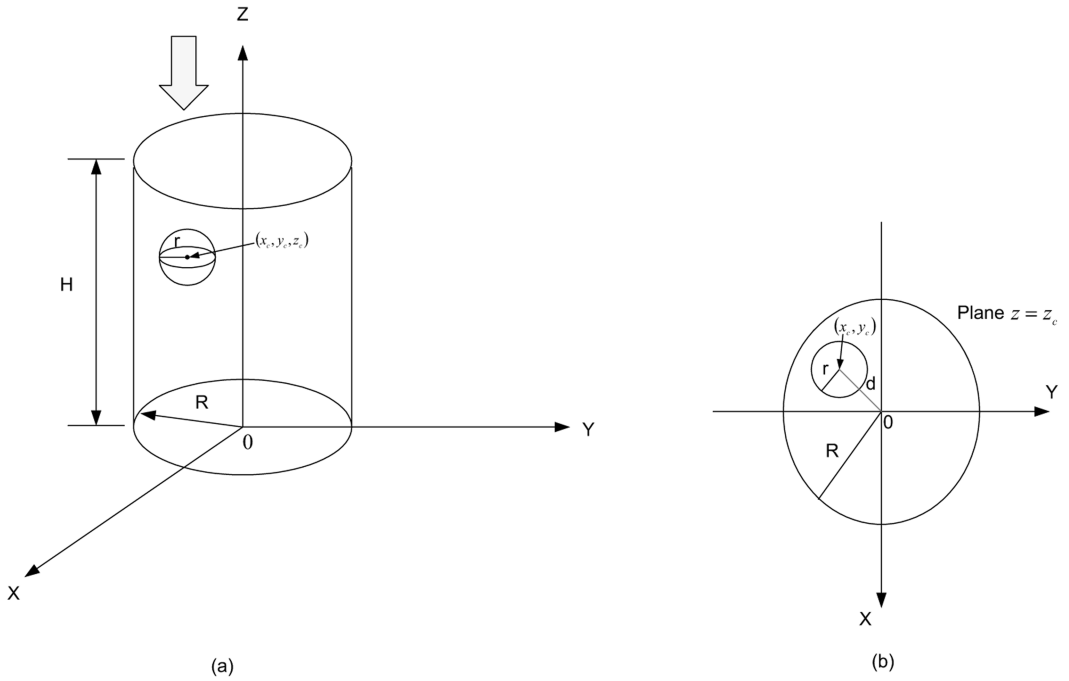

Fig. 7 Intersection of the sphere and the cylindrical surface

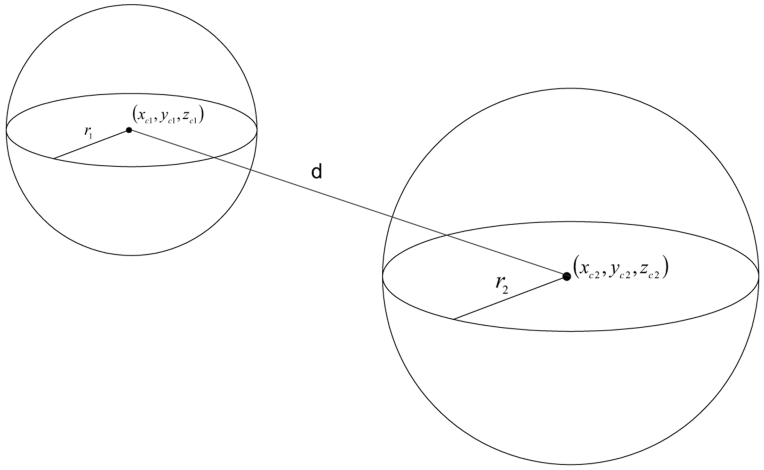

Fig. 8 Representation of two spheres

minimum distance $D_{\min}$ from the surface. Therefore, the equation for checking the minimum distance between the sphere and the surface is given by

$$R-(d+r)\geq D_{\min} \tag{50}$$

3.2.2. Two spheres

Intersection: Given two spheres, S_1 and S_2 characterized by center point (x_{ci}, y_{ci}, z_{ci}) and radius

(r_i), Fig. 8. It must be verified that S_2 is not entirely inside S_1. If the center of S_1 is contained in S_2, S_1 intersects S_2. If the center of S_1 lies outside S_2, then S_1 intersects S_2 if and only if the surfaces intersects.

• Sphere embedded into another: We first check if the center of S_1 is inside S_2. From Eq. (9) we obtain

$$f = (x-x_{c2})^2 + (y-y_{c2})^2 + (z-z_{c2})^2 \tag{51}$$

and hence, to determine whether the center of S_1 isinside S_2, we evaluate f from Eq. (51) by substituting x, y and z with x_{c1}, y_{c1} and z_{c1}, respectively. If f is less than or equal to r_2, the center of S_1 is inside S_2, otherwise, it is outside.

• S_1 and S_2 are separated if the center of an sphere is not inside the other one, then to test for intersection it can be done by calculating the distance between their centers and then comparing it to the sum of the radii. The two spheres intersect if

$$\sqrt{(x_{c1}-x_{c2})^2 + (y_{c1}-y_{c2})^2 + (z_{c1}-z_{c2})^2} \le r_1 + r_2 \tag{52}$$

Distance: Next we seek to check the minimum distance between the two shperes S_1 and S_2 which should have a minimum distance of $D_{\min}$ if

$$\sqrt{(x_{c1}-x_{c2})^2 + (y_{c1}-y_{c2})^2 + (z_{c1}-z_{c2})^2} - (r_1 + r_2) \ge D_{\min} \tag{53}$$

4. Adjusting particle location

If a particle collides with the matrix boundaries or with another ellipse (in 2D) or ellipsoid (in 3D), then it must be repositioned such that the distance between the two entities d is larger than $D_{\min}$.

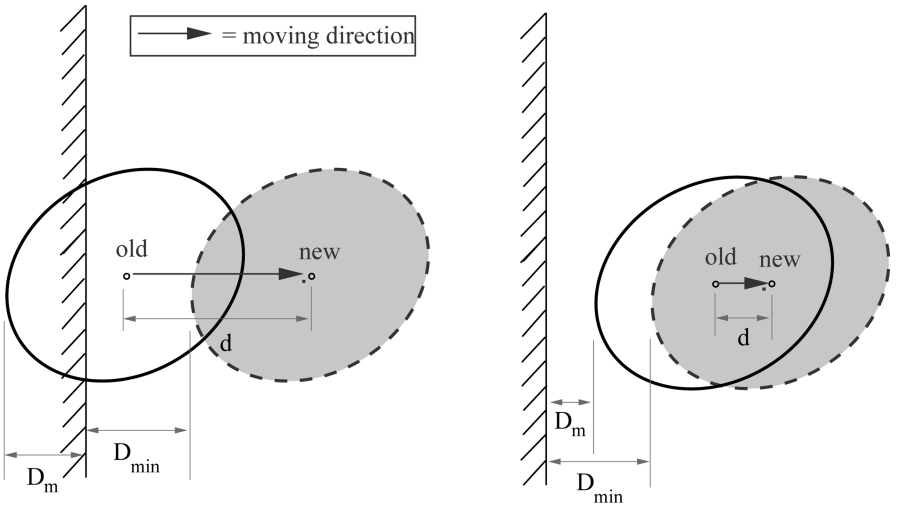

a) if particle intersects with matrix boundary

b) if distance between particle and matrix boundary D_m is less than D_{min}

Fig. 9 Moving direction away from matrix boundary

4.1. With respectto matrix boundary

In the first case, we consider adjustment if a particle collides with the boundary of the matrix. The particle will be shifted to a new position in the direction orthogonal to the boundary. If we wish to translate the ellipse or the ellipsoid by a distance d away from the matrix boundary (in terms of $D_{\min}$ and D_m which are the minimum allowable and the old distance between particle and matrix boundary respectively), then d can be obtained from, Fig. 9,

$$d = \begin{Bmatrix} D_m + D_{\min}(\text{Case a}) \\ D_{\min} - D_m(\text{Case b}) \end{Bmatrix} \tag{55}$$

4.2. With respect to another particle

In the second case, we consider adjustment if a particle collides with another or if the shortest distance between particles is less than the minimum allowable one. The particle will be shifted along the direction of the shortest distance between the boundaries. Thus, if we need to shift a particle by a distance d, and D_e is the shortest distance between particles at the old position and $D_{\min}$ the minimum allowable distance, then from Fig. 10, d can be determined from

$$d = \begin{Bmatrix} D_e + D_{\min}(\text{Case a}) \\ D_{\min} - D_e(\text{Case b}) \end{Bmatrix} \tag{55}$$

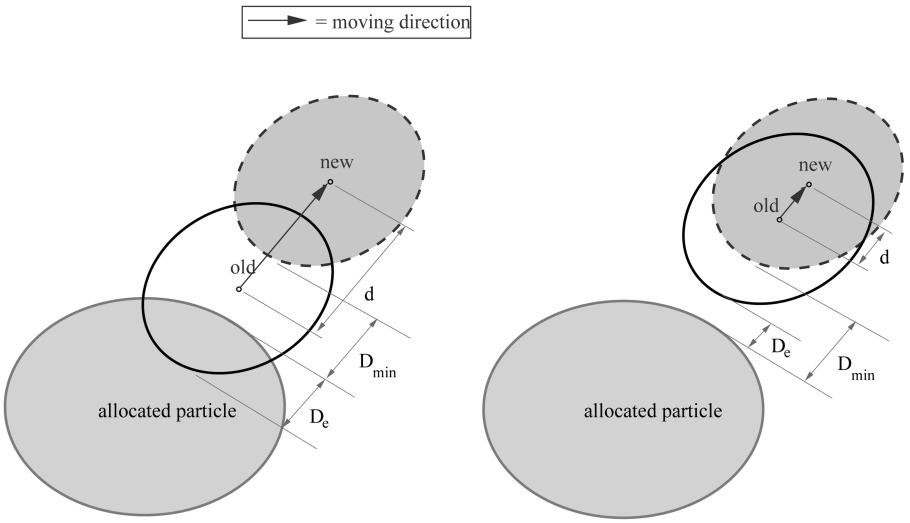

Fig. 10 Moving dircetion away from the allocated particle

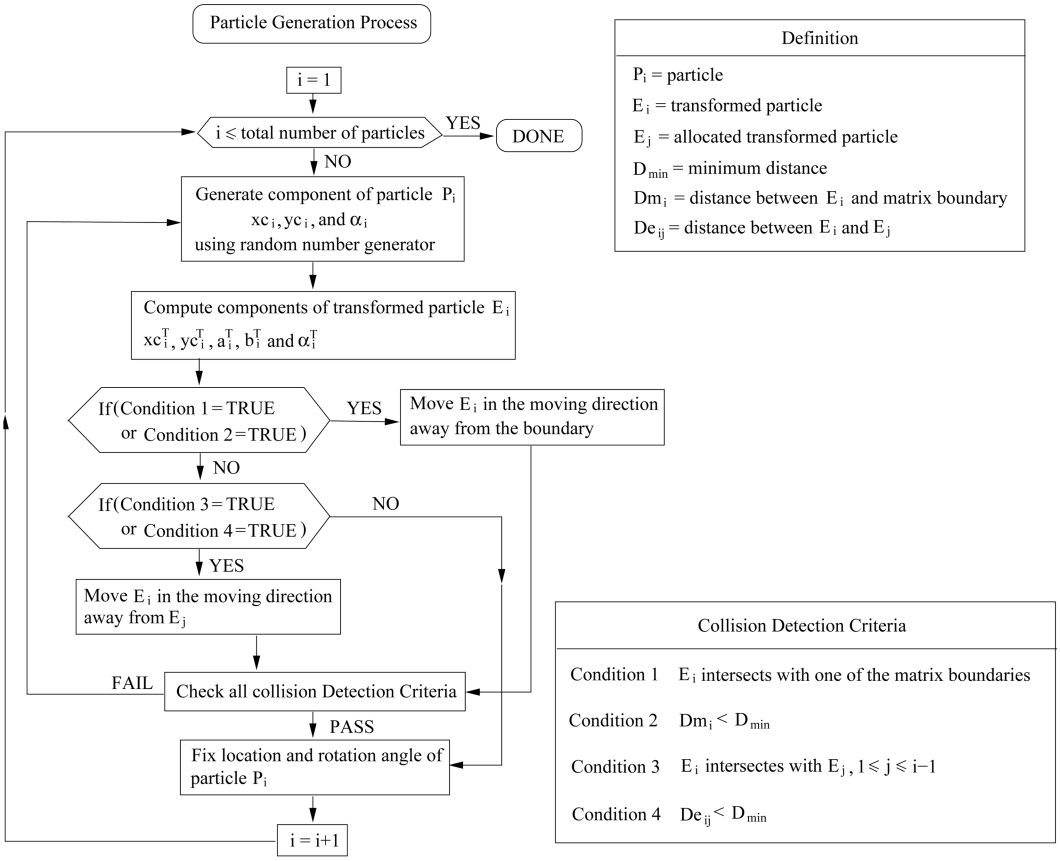

Fig. 11 Particle generation algorithm (2D example)

5. Particle placement algorithm

Following the preceding coverage, we now present the actual algorithm for random placement of particles inside a matrix, Fig. 11.

6. Computer implementation

The various algorithms previously presented have been programmed in C++ in a Windows based application (PARSIFAL, PARticle Simulator For AnaLysis). This application is the program used to generate hetero-geneous material model in RVE, and then it can be used to generate finite difference grid or finite element meshes through tools such as T3D, (Rypl 1998). Fig. 12 illustrated the mesh generation process in 2D.

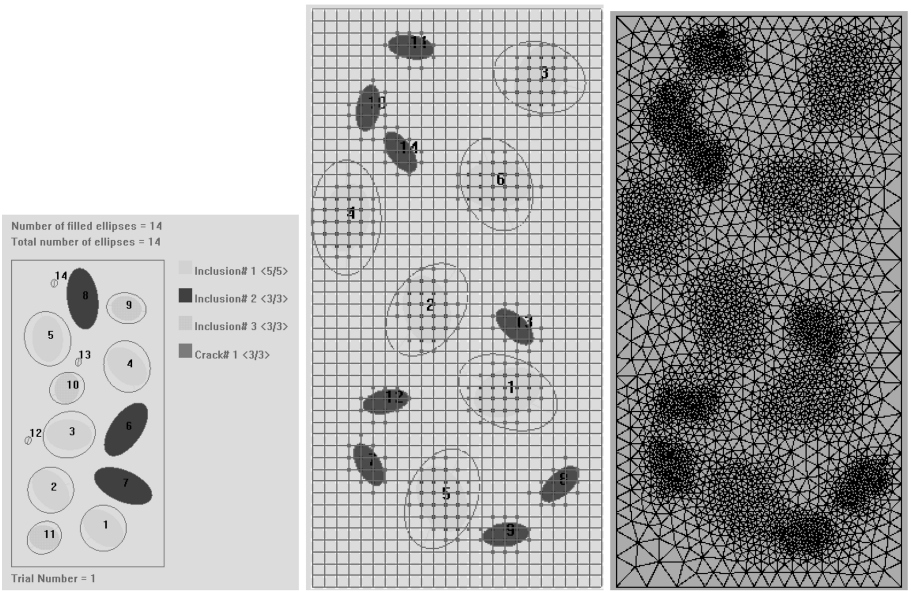

Fig. 12 Particle definition and corresponding finite difference grid and finite element mesh in 2D

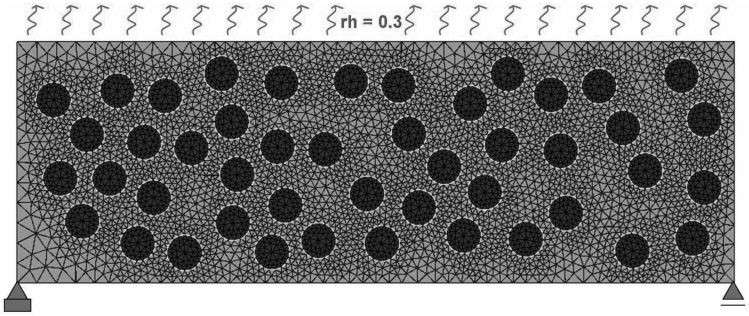

Fig. 13 Mesh and boundary conditions used in the simulation

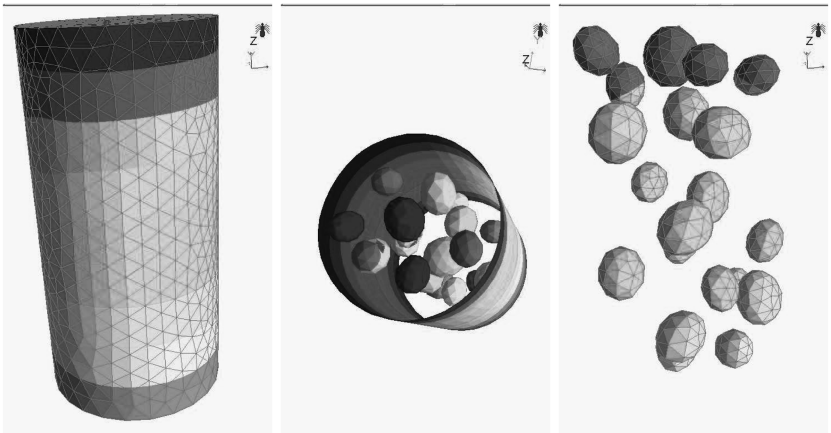

Fig. 14 3D Finite element mesh

7. Application

A 2D example of application for the developed mesh generation algorithm is the meso-mechanical simulation of drying shrinkage in concrete, (Segura and Carol 2004). Fig. 13 illustrates the original mesh with the top surface exposed to 30% relative humidity while the other sides remain sealed. Mono-size circular aggregates have been generated with adiameter of 6 mm (aggregate volume fraction equal to27% of the total volume).

Another application is the meso-mechanics investigation of a concrete cylinder with 20 elliptical aggre-gates. The 300 by 150 mm cylinder has an 11% fraction of aggregates with a Young modulus ten times higher the one of the cement paste. As a result the effective Young modulus is 13.6% higher than the one of the cement paste. This is close to the theoretical increase of 9.5% for spherical inclusions (Christensen 1979).

8. Conclusions

The mathematical procedure to implement a numerical model for a representative volume element of hetero-geneous materials (such as concrete) is presented. The model idealizes particle as either ellipses or ellipsoids (2D and 3D respectively) which can be randomly placed in a rectangular or cylindrical environment.

A numerical example for the simulation of dry shrinkage of concrete, using a finite element mesh generated by the proposed procedure, is presented.

Acknowledgments

The first author would like to acknowledge the support of the Department of Civil Engineering, Faculty of Engineering, Ubon Ratchathani University, Thailand. The authors would like to thank Mr. Andres Idiart from the Polytechnic University of Catalunya for providing the numerical shrinkage simulation example.

References

Carol, I. and López, Roa, O. (2001), "Micromechanical analysis of quasi-brittle materials using fracture-based interface elements", *Int. J. Numer. Meth. Eng*., **52**(1-2), 193-215.

Christensen, R. (1979), *Mechanics of Composite Materials*, Wiley Interscience, New York.

Cusatis, G., Bažant, Z. and Cedolin, L. (2003), "Confinement-shear lattice model for concrete damage in tension and compression: I. theory", A*SCE J. Eng. Mech.* **129**(12), 1439-1448.

Fuller, W. and Thompson, S. (1907), "The laws of proportioning concrete", *Trans. Am. Soc. Civ. Eng*., **59**, 67-7143. Paper Number 1053.

Hsu, T., Slate, F., Sturman, G. and Winter, G. (1963), "Microcracking of plain concrete and the shape of the stress-strain curve", *J. American Concrete Institute*, **60**, 209-224.

Leite, J., Slowik, V. and Apel, J. (2007), "Computational model of mesoscopic structure of concrete for simulation of fracture processes", *Comput. Struct.* **85**, 1293-1303.

Press, W., Flannery, B., Teukolvsky, S. and Vetterling, W. (1988), *Numerical Recipes in C, The Art of Scientific Computing*, Cambridge University Press.

Roberts, A. and Garboczi, E. (2002), "Computation of the linear elastic properties of random porous materials with a wide variety of microstructure", *Proc. Royal Soc. of London* **458**, 1033-1054.
Roelfstra, P. E. and Sadouki, H. and Wittmann, F. H. (1985), "Numerical concrete", *Mater. Struct.* **18**, 327-335.
Rypl, D. (1998), "Sequential and parallel generation of unstructured 3D meshes", PhD thesis, Czech Technical University in Prague. http://ksm.fsv.cvut.cz/~dr/t3d.html.
Segura, J. and Carol, I. (2004), "On zero-thickness interface elements for diusion problems", *Int. J. Numer. Analytical Meth. Geomech.* **28**(9), 947-962.
Slate, F. and Olsefski, S. (1963), "X-rays for study of internal structures and microcracking of concrete", *J. the American Concrete Institute* **60**, 575-587.
Willam, K., Rhee, I. and Xi, Y. (2005), "Thermal degradation of heterogeneous concrete materials", ASCE *J. Mater. Civ. Eng.* **17**(3), 276-285.
Willam, K., Stankowski, T., Weihe, S., Runesson, K. and Sture, S. (1989), "Simulation issues of distributed and localized failure computations", in J. Mazars and Z. P. Bažant (eds), *Cracking and Damage-Strain Localization and Size Eect*, Elsevier Appl. Science, pp.363-378.
Zheng, J., Li, C. and Zhao, L. (2003), "Simulation of two-dimensional aggregate distribution with wall effect", *J. Mater. Civ. Eng.* **15**(5), 506-510.

CM